4-1-2013

SR-Like RNA-binding protein Slr1 affects Candida albicans filamentation and virulence

Chaiyaboot Ariyachet
Bowdoin College

Norma V. Solis
The Lundquist Institute

Yaoping Liu
The Lundquist Institute

Nemani V. Prasadarao
Keck School of Medicine of USC

Scott G. Filler
The Lundquist Institute

See next page for additional authors

IAI Journals.ASM.org

SR-Like RNA-Binding Protein Slr1 Affects *Candida albicans* Filamentation and Virulence

Chaiyaboot Ariyachet,[a]* Norma V. Solis,[b] Yaoping Liu,[b] Nemani V. Prasadarao,[c] Scott G. Filler,[b,d] Anne E. McBride[a]

Department of Biology, Bowdoin College, Brunswick, Maine, USA[a]; Los Angeles Biomedical Research Institute at Harbor-UCLA Medical Center, Torrance, California, USA[b]; Division of Infectious Diseases, The Saban Research Institute, Children's Hospital Los Angeles, and Keck School of Medicine, University of Southern California, Los Angeles, California, USA[c]; David Geffen School of Medicine at UCLA, Los Angeles, California, USA[d]

Candida albicans **causes both mucosal and disseminated infections, and its capacity to grow as both yeast and hyphae is a key virulence factor. Hyphal formation is a type of polarized growth, and members of the SR (serine-arginine) family of RNA-binding proteins influence polarized growth of both *Saccharomyces cerevisiae* and *Aspergillus nidulans*. Therefore, we investigated whether SR-like proteins affect filamentous growth and virulence of *C. albicans*. BLAST searches with *S. cerevisiae* SR-like protein Npl3 (ScNpl3) identified two *C. albicans* proteins: CaNpl3, an apparent ScNpl3 ortholog, and Slr1, another *S*R-*l*ike *R*NA-binding protein with no close *S. cerevisiae* ortholog. Whereas ScNpl3 was critical for growth, deletion of *NPL3* in *C. albicans* resulted in few phenotypic changes. In contrast, the *slr1*Δ/Δ mutant had a reduced growth rate *in vitro*, decreased filamentation, and impaired capacity to damage epithelial and endothelial cells *in vitro*. Mice infected intravenously with the *slr1*Δ/Δ mutant strain had significantly prolonged survival compared to that of mice infected with the wild-type or *slr1*Δ/Δ mutant complemented with *SLR1* (*slr1*Δ/Δ+*SLR1*) strain, without a concomitant decrease in kidney fungal burden. Histopathology, however, revealed differential localization of *slr1*Δ/Δ hyphal and yeast morphologies within the kidney. Mice infected with *slr1*Δ/Δ cells also had an increased brain fungal burden, which correlated with increased invasion of brain, but not umbilical vein, endothelial cells *in vitro*. The enhanced brain endothelial cell invasion was likely due to the increased surface exposure of the Als3 adhesin on *slr1*Δ/Δ cells. Our results indicate that Slr1 is an SR-like protein that influences *C. albicans* growth, filamentation, host cell interactions, and virulence.**

The opportunistic pathogen *Candida albicans* is a multimorphic fungus that is a leading cause of nosocomial bloodstream infections in the United States (1). *C. albicans* can adopt at least three morphologies, a budding yeast form and two filamentous forms, hyphae and pseudohyphae, which result from polarized cell growth. The ability of *C. albicans* to switch between yeast and hyphal morphologies has been implicated in virulence in various model systems (2, 3). Compared to *C. albicans* yeast cells, hyphae have a greater capacity to adhere to and invade host cells (4). Epithelial cell invasion leads to the establishment of mucosal infections, as seen in oropharyngeal and vulvovaginal candidiasis, whereas internal organ infection during disseminated disease requires *C. albicans* cells to penetrate through the endothelial lining of the vasculature. Given the link between the yeast-hyphal transition and virulence, many studies have explored changes in gene expression during the switch to polarized hyphal growth and the signaling pathways and transcription factors required for this transition (5–9). To date, however, less attention has been focused on posttranscriptional regulation of gene expression in *C. albicans* morphological switching (10–13).

In numerous eukaryotic systems, posttranscriptional processes are critical for establishing polarity and are frequently controlled by mRNA sequences outside the open reading frame (14–16). Transcriptome analysis of *C. albicans* recently revealed numerous long 5′ and 3′ untranslated regions (UTRs) and confirmed the presence of more than 400 introns (7, 8, 17), which indicate opportunities for posttranscriptional regulation of gene expression. Three proteins involved in mRNA decay have been linked to *C. albicans* morphogenesis to date. Strains lacking the 5′-to-3′ exonuclease Kem1/Xrn1 display altered hyphal growth (10) and defects in intermediate stages of biofilm formation (11). Deletion of the mRNA deadenylase components Ccr4 and Pop2 also results in filamentation defects (13). In addition, the She3 mRNA-binding protein binds to and directs hyphal tip localization of specific mRNAs, and absence of this protein affects filamentous growth on solid media (12).

The SR (serine-arginine) family of RNA-binding proteins has been implicated in many steps of mRNA metabolism across eukaryotes. First identified as constitutive and regulated splicing factors, SR proteins are now known to have multiple roles, including linking transcription to splicing, nuclear mRNA export, and translational regulation (18–20). Fungal genomes encode proteins that are structurally similar to SR proteins, and the major SR-like protein in *Saccharomyces cerevisiae*, Npl3, plays numerous roles in mRNA metabolism (21–26). Interestingly, deletion of Npl3 causes polarity defects—in diploid bud-site selection and in the switch from budding to pseudohyphal growth in haploid cells (27, 28). We therefore sought to identify SR-like proteins in *C. albicans* that

Received 16 August 2012 **Returned for modification** 3 September 2012
Accepted 25 January 2013
Published ahead of print 4 February 2013
Editor: G. S. Deepe, Jr.
Address correspondence to Anne E. McBride, amcbride@bowdoin.edu.
* Present address: Chaiyaboot Ariyachet, Department of Stem Cell and Regenerative Biology, Harvard University, Cambridge, Massachusetts, USA.
Supplemental material for this article may be found at http://dx.doi.org/10.1128/IAI.00864-12.

doi:10.1128/IAI.00864-12

might be involved in posttranscriptional processes that affect morphogenesis. Our search for SR-like proteins similar to Npl3 in *C. albicans* revealed that the protein most similar to *S. cerevisiae* Npl3 contained only a single SR dipeptide (29). A second protein, which we have named *S*R-*l*ike *R*NA-binding protein 1 (Slr1), shows sequence similarity not only to Npl3 but also to the *Schizosaccharomyces pombe* SR protein Srp1 and to the *Aspergillus nidulans* protein SwoK, the latter of which has been implicated in polarized growth (30).

Here we describe the characterization of Slr1 in *C. albicans* and its importance for *C. albicans* growth, filamentation, and virulence. Decreased growth and filamentation of cells lacking Slr1 *in vitro* correlated with reduced virulence in a mouse model of disseminated infection, yet this strain displayed a kidney fungal burden equivalent to that for wild-type *C. albicans*, as well as a greater fungal burden in the brain. The increased ability of cells lacking Slr1 to invade brain endothelial cells *in vitro* and greater surface exposure of the hypha-specific Als3 adhesin protein on *slr1*Δ/Δ cells likely contributed to its increased brain tropism in mice. These results indicate that Slr1 is involved in processes that are important for both filamentation and virulence of *C. albicans* in the mammalian host.

MATERIALS AND METHODS

Strain construction. Genotypes of strains used in this study are found in Table 1. All *C. albicans* strains in this study are derived from strain BWP17 and were created using a lithium acetate-based transformation protocol (31). All strains used in growth and virulence studies were prototrophic for arginine and histidine and contained the *URA3* gene at its native locus (32). Strain construction is described in the supplemental material and important features of plasmids and oligonucleotides are found in Tables S1 and S2.

***In vitro* growth assays.** To determine the maximal growth rate in liquid culture, indicated strains (5 to 10 replicates, including independently isolated mutant and reconstituted strains) were inoculated into 300 μl yeast extract-peptone-dextrose (YPD) in a 96-deep-well plate and grown overnight (23 to 27 h). Cells were diluted 1,000-fold into 150 μl YPD in flat-bottom 96-well dishes, and growth was monitored in a Tecan Sunrise (San Jose, CA) microplate reader. Cultures were shaken at 30°C or 37°C for 24 h, and optical density at 600 nm was monitored every 15 min. Optical density data were exported to the Excel software program using Magellan data analysis software and subsequently analyzed using growth curve analysis software, kindly provided by Darren Abbey and Sven Bergmann. This Matlab script fits the logistic growth curve to the data for a single well and then calculates the generation time for each sample at its maximal growth rate based on this fit (33, 34). Mean generation times were calculated for each strain.

To test for sensitivity to cell wall and cell membrane stressors, strains were grown overnight in YPD broth (1% yeast extract, 2% Bacto peptone, and 2% glucose), diluted into fresh YPD broth the following morning, and plated after 6 h of growth. Cells were washed and resuspended in phosphate-buffered saline (PBS), and 5×10^4 and 5×10^3 cells were spotted onto YPD agar with or without 0.2% sodium dodecyl sulfate (SDS) or 20 μM calcofluor white and grown for 1 day at 30°C.

Filamentation on solid medium was tested by plating 10^7 stationary-phase cells on plates containing 2% agar and 5% fetal bovine serum or 1.5% agar and 1× RPMI 1640 medium (Invitrogen 31800 with L-glutamine; pH adjusted to 7.5 with HEPES) or on solid Spider medium (data not shown) (35). Colonies were photographed after 6 days of incubation at 37°C. To test filamentation in liquid culture, cells from overnight cultures grown in YPD broth at 30°C were washed, diluted to 10^5 cells/ml in prewarmed RPMI 1640 medium without L-glutamine (Irving Scientific), and added to sterile, 12-mm, gelatin-coated glass coverslips in a 24-well tissue culture plate. The cells were incubated in 5% CO_2 at 37°C for 1.5 or 3 h, fixed with 3% paraformaldehyde, and imaged by differential-interference contrast microscopy.

Host cells. The FaDu oral epithelial cell line was obtained from the American Type Culture Collection and grown as recommended by the supplier. Human umbilical vein endothelial cells (HUVECs) were harvested by the method of Jaffe et al. (36) and grown as described previously (37). Human brain microvascular endothelial cells (HBMECs) were grown as described previously (38, 39).

Host cell damage assay. The capacities of the different *C. albicans* strains to damage the FaDu oral epithelial cell line, HUVECs, and HBMECs were determined by a ^{51}Cr release assay as previously outlined (37). Briefly, the host cells were grown to 90% confluence in 96-well tissue culture plates, loaded with ^{51}Cr overnight, and then inoculated with yeast-phase *C. albicans* cells. For experiments with FaDu cells, the inoculum was 1×10^5 *C. albicans* cells per well suspended in RPMI 1640 medium without L-glutamine (Irvine Scientific), and the incubation period was 3 h. For HUVECs, the inoculum was 4×10^4 *C. albicans* cells per well in RPMI 1640 medium, and the incubation period was 3 h (40). Because HBMECs were resistant to *C. albicans*-induced damage, the inoculum was 1×10^5 *C. albicans* cells per well in Ham's F-12K medium, and the incubation period was increased to 16 h. At the end of the incubation period, the medium above the cells was collected, and the ^{51}Cr content was determined by γ counting. Damage assays for each host cell type were performed in triplicate on three separate occasions with the wild-type (AMC81), *slr1*Δ/Δ mutant (AMC82), and *slr1*Δ/Δ mutant complemented with *SLR1* (*slr1*Δ/Δ+*SLR1*) (AMC104) strains.

Endocytosis assay. Endocytosis by HUVECs and HBMECs of the different *C. albicans* strains was assessed using a differential fluorescence assay as described previously (39). Each type of endothelial cell was grown on fibronectin-coated glass coverslips in 24-well tissue culture plates and then infected with 10^5 *C. albicans* yeast cells in RPMI 1640 medium. After 3 h of incubation, the cells were fixed with 3% paraformaldehyde, after which the noninternalized cells were stained with anti-*C. albicans* rabbit serum (Biodesign International) conjugated with Alexa 568 (Invitrogen). Next, the endothelial cells were permeabilized in 0.1% (vol/vol) Triton X-100 in PBS, and then both the internalized and noninternalized organisms were stained with anti-*C. albicans* rabbit serum conjugated with Alexa Fluor 488 dye (Invitrogen). The coverslips were viewed using an epifluorescence microscope (Axiovert 10; Carl Ziess, Inc.), and the number of organisms endocytosed by the endothelial cells was determined by subtracting the number of noninternalized organisms (which fluoresced red) from the total number of organisms (which fluoresced green). More than 100 organisms were counted on each coverslip, and the experiments were performed in triplicate on three separate occasions.

Virulence studies. The relative virulences of the various *C. albicans* strains were determined using mouse models of hematogenously disseminated candidiasis (HDC) (41) and oropharyngeal candidiasis (OPC) (42, 43) using male ICR mice (Taconics Farms). In the HDC model, eight mice per strain were injected via the tail vein with 7.5×10^5 yeast and monitored for survival over a 3-week period. Seven or eight additional mice were similarly infected and sacrificed after 4 days, after which the fungal burdens of the kidney, liver, and brain were analyzed by quantitative culture as previously described (39). The histopathology of a kidney from each mouse was examined by periodic acid-Schiff staining (44). A second survival study was also performed with an *slr1*Δ/Δ mutant generated from an independent *slr1*Δ/*SLR1* heterozygous strain and a corresponding reconstituted strain, as well as the wild-type strain, using 10 mice per strain and the same inoculum.

In the OPC model, 6 to 7 mice per *C. albicans* strain were immunosuppressed with cortisone acetate (200 mg/kg of body weight; Sigma-Aldrich) administered subcutaneously on days −1, 1, and 3 relative to infection. On the day of infection, the mice were sedated with ketamine and xylaxine, after which a calcium alginate swab saturated with 10^6 *C. albicans* yeast cells was placed sublingually for 75 min. After 5 days of

TABLE 1 Strains used in this study

Strain	Genotypes[a]	Parental strain or reference
AMC8	***npl3Δ::ARG4*** *ura3Δ::λimm434 arg4::hisG his1::hisG* ***NPL3*** *ura3Δ::λimm434 arg4::hisG his1::hisG*	BWP17
AMC18	***npl3Δ::HIS1*** *ura3Δ::λimm434::**URA3-IRO1** arg4::hisG his1::hisG* ***npl3Δ::ARG4*** *ura3Δ::λimm434 arg4::hisG his1::hisG*	AMC37
AMC20	***npl3Δ::HIS1*** *ura3Δ::λimm434::**URA3-IRO1** arg4::hisG his1::hisG* ***npl3Δ::ARG4*** *ura3Δ::λimm434 arg4::hisG his1::hisG*	AMC38
AMC22	***npl3Δ::HIS1::NPL3*** *ura3Δ::λimm434::**URA3-IRO1** arg4::hisG his1::hisG* ***npl3Δ::ARG4*** *ura3Δ::λimm434 arg4::hisG his1::hisG*	AMC18
AMC24	***npl3Δ::HIS1::NPL3*** *ura3Δ::λimm434::**URA3-IRO1** arg4::hisG his1::hisG* ***npl3Δ::ARG4*** *ura3Δ::λimm434 arg4::hisG his1::hisG*	AMC20
AMC37	***npl3Δ::HIS1*** *ura3Δ::λimm434 arg4::hisG his1::hisG* ***npl3Δ::ARG4*** *ura3Δ::λimm434 arg4::hisG his1::hisG*	AMC8
AMC38	***npl3Δ::HIS1*** *ura3Δ::λimm434 arg4::hisG his1::hisG* ***npl3Δ::ARG4*** *ura3Δ::λimm434 arg4::hisG his1::hisG*	AMC8
AMC67	***slr1Δ::ARG4*** *ura3Δ::λimm434 arg4::hisG his1::hisG* ***SLR1*** *ura3Δ::λimm434 arg4::hisG his1::hisG*	BWP17
AMC68	***slr1Δ::HIS1*** *ura3Δ::λimm434::**URA3-IRO1** arg4::hisG his1::hisG* ***slr1Δ::ARG4*** *ura3Δ::λimm434 arg4::hisG his1::hisG*	AMC90
AMC70	***slr1Δ::HIS1*** *ura3Δ::λimm434::**URA3-IRO1** arg4::hisG his1::hisG* ***slr1Δ::ARG4*** *ura3Δ::λimm434 arg4::hisG his1::hisG*	AMC89
AMC71	***slr1Δ::hisG*** ***npl3Δ::HIS1*** *ura3Δ::λimm434 arg4::hisG his1::hisG* ***SLR1*** ***npl3Δ::ARG4*** *ura3Δ::λimm434 arg4::hisG his1::hisG*	AMC37
AMC72	***slr1Δ::hisG*** ***npl3Δ::HIS1*** *ura3Δ::λimm434 arg4::hisG his1::hisG* ***slr1Δ::hisG*** ***npl3Δ::ARG4*** *ura3Δ::λimm434 arg4::hisG his1::hisG*	AMC71
AMC81	***ura3Δ::λimm434::URA3-IRO1*** ***arg4::hisG::ARG4*** ***his1::hisG::HIS1*** *ura3Δ::λimm434 arg4::hisG his1::hisG*	BWP17
AMC82	***slr1Δ::HIS1*** *ura3Δ::λimm434::**URA3-IRO1** arg4::hisG his1::hisG* ***slr1Δ::ARG4*** *ura3Δ::λimm434 arg4::hisG his1::hisG_*	AMC89
AMC83	***slr1Δ::hisG*** ***npl3Δ::HIS1*** *ura3Δ::λimm434::URA3-IRO1 arg4::hisG his1::hisG* ***slr1Δ::hisG*** ***npl3Δ::ARG4*** *ura3Δ::λimm434 arg4::hisG his1::hisG*	AMC72
AMC87	***slr1Δ::HIS1*** *ura3Δ::λimm434 arg4::hisG his1::hisG* ***SLR1*** *ura3Δ::λimm434 arg4::hisG his1::hisG*	BWP17
AMC89	***slr1Δ::HIS1*** *ura3Δ::λimm434 arg4::hisG his1::hisG* ***slr1Δ::ARG4*** *ura3Δ::λimm434 arg4::hisG his1::hisG*	AMC87
AMC90	***slr1Δ::ARG4*** *ura3Δ::λimm434 arg4::hisG his1::hisG* ***slr1Δ::HIS1*** *ura3Δ::λimm434 arg4::hisG his1::hisG*	AMC67
AMC103	***slr1Δ::ARG4::SLR1*** *ura3Δ::λimm434::**URA3-IRO1** arg4::hisG his1::hisG* ***slr1Δ::HIS1*** *ura3Δ::λimm434 arg4::hisG his1::hisG*	AMC89
AMC104	***slr1Δ::ARG4::SLR1*** *ura3Δ::λimm434::**URA3-IRO1** arg4::hisG his1::hisG* ***slr1Δ::HIS1*** *ura3Δ::λimm434 arg4::hisG his1::hisG*	AMC89
AMC105	***slr1Δ::ARG4::SLR1*** *ura3Δ::λimm434::**URA3-IRO1** arg4::hisG his1::hisG* ***slr1Δ::HIS1*** *ura3Δ::λimm434 arg4::hisG his1::hisG*	AMC90

(Continued on following page)

TABLE 1 (Continued)

Strain	Genotypes[a]	Parental strain or reference
AMC110	***slr1Δ::hisG npl3Δ::HIS1*** *ura3Δ::λimm434::**URA3-IRO1*** *arg4::hisG his1::hisG* ***slr1Δ::hisG npl3Δ::ARG4*** *ura3Δ::λimm434 arg4::hisG his1::hisG*	AMC72
AMC111	***slr1Δ::hisG::SLR1*** ***npl3Δ::HIS1*** *ura3Δ::λimm434::**URA3-IRO1*** *arg4::hisG his1::hisG* ***slr1Δ::hisG*** ***npl3Δ::ARG4*** *ura3Δ::λimm434 arg4::hisG his1::hisG*	AMC72
AMC112	***slr1Δ::hisG::SLR1*** ***npl3Δ::HIS1*** *ura3Δ::λimm434::**URA3-IRO1*** *arg4::hisG his1::hisG* ***slr1Δ::hisG*** ***npl3Δ::ARG4*** *ura3Δ::λimm434 arg4::hisG his1::hisG*	AMC72
AMC113	***slr1Δ::hisG npl3Δ::HIS1::NPL3*** *ura3Δ::λimm434::**URA3-IRO1*** *arg4::hisG his1::hisG* ***slr1Δ::hisG npl3Δ::ARG4*** *ura3Δ::λimm434 arg4::hisG his1::hisG*	AMC72
AMC114	***slr1Δ::hisG npl3Δ::HIS1::NPL3*** *ura3Δ::λimm434::**URA3-IRO1*** *arg4::hisG his1::hisG* ***slr1Δ::hisG npl3Δ::ARG4*** *ura3Δ::λimm434 arg4::hisG his1::hisG*	AMC72
BWP17	*ura3Δ::λimm434 arg4::hisG his1::hisG* *ura3Δ::λimm434 arg4::hisG his1::hisG*	31
DAY185	*ura3Δ::λimm434* ***ARG4::URA3::arg4::hisG*** ***HIS1::his1::hisG*** *ura3Δ::λimm434 arg4::hisG his1::hisG*	59

[a] Boldface indicates differences from the parental strain, BWP17. For each strain, each gene is underlined and the two alleles of the gene are listed in the upper and lower rows.

infection, the mice were sacrificed, and then their tongues were harvested, weighed, and homogenized. *C. albicans* cells in homogenized tissue were quantified by culture on solid on Sabouraud dextrose agar containing 10 μg/ml chloramphenicol (34).

Flow cytometry. To assess the level of Als3 expression on the surface of the various strains, the organisms were germinated for 90 min in liquid RPMI 1640 medium containing 10% fetal bovine serum at 37°C. The resulting germ tubes were fixed in 3% paraformaldehyde and blocked with normal goat serum. Surface-exposed Als3 was detected by staining with a polyclonal rabbit anti-Als3 primary antibody (37) followed by an Alexa Fluor 488-labeled goat anti-mouse secondary antibody. The amount of Als3 staining was quantified by flow cytometry.

Statistics. Differences in the generation times between different *C. albicans* strains *in vitro* were determined by analysis of variance with a Tukey posttest. Differences in the host cell interactions among the various *C. albicans* strains *in vitro* were evaluated by analysis of variance. Differences in the survival of mice infected with the different strains were analyzed by the log rank test, and differences in organ fungal burden were assessed using the Wilcoxon rank sum test.

RESULTS

Identification of SR-like proteins in *C. albicans*. A BLAST search of the *C. albicans* genome with the ScNpl3 sequence revealed two proteins with strong similarity to Npl3 (Fig. 1). The apparent *C. albicans* Npl3 ortholog (CaNpl3) shares a core domain structure with SpSrp2 and with ScNpl3: two *R*NA *r*ecognition *m*otifs (RRMs), followed by an arginine-rich domain (Fig. 1). Each protein, however, contains features not seen in the other two proteins. ScNpl3 has an additional N-terminal domain that the other two proteins lack. The arginine-rich domain of SpSrp2 is less repetitive than those of the Npl3 proteins and is followed by a higher-complexity C-terminal region not found in the Npl3 proteins. Whereas the arginine-rich domains of SpSrp2 and ScNpl3 contain multiple serine-arginine (SR) or arginine-serine (RS) dipeptides, CaNpl3 has only a single SR dipeptide, which is found at the C terminus of the protein in the heptapeptide RER**S**PTR.

The *S. cerevisiae* genome contains no apparent ortholog of the *S. pombe* SR-like protein (SpSrp1) gene *SRP1* (45), but *ORF19.1750* in *C. albicans* encodes an SR-like protein with a domain structure similar to that of SpSrp1: a single RRM followed by a long arginine-rich region (Fig. 1). Reciprocal BLASTP searches of the *C. albicans* and *S. pombe* proteomes using the RRM sequences from each protein indicate a strong sequence similarity in these regions. Based on this similarity, we have named *ORF19.1750* *S*R-*l*ike *R*NA-binding protein *1* (*SLR1*). Both the *SpSRP1* and *C. albicans SLR1* (*CaSLR1*) genes contain introns, and the location of the 5′ splice site for the first intron is the same in the two genes, occurring 44 nucleotides downstream of the final codon of the RNP-2 motif within the RRM, suggesting an evolutionary relationship between these genes. BLASTP searches with the RRM domains of CaSlr1 and SpSrp1 revealed similar proteins in numerous fungal lineages, but no apparent orthologs were found in *Zygosaccharomyces rouxii*, *Vanderwaltozyma polyspora*, or *Saccharomyces* species.

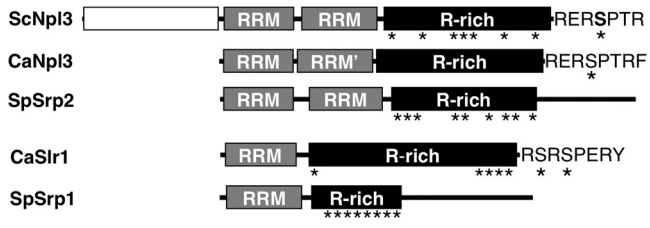

FIG 1 *C. albicans* proteins similar to *S. cerevisiae* and *S. pombe* SR-like proteins. In domain comparison of two SR-like proteins in *Saccharomyces cerevisiae*, *Schizosaccharomyces pombe*, and *Candida albicans*, RNA recognition motifs (RRM) and arginine-rich (R-rich) domains, as well as nonconserved N- and C-terminal domains, are shown. Asterisks indicate locations of SR/RS dipeptides. The second domain of the *C. albicans* Npl3-like protein (RRM′) has sequence similarity with the other two atypical RRMs in ScNpl3 and SpSrp2 but is not recognized as an RRM by protein signature recognition searches (InterProScan). GenBank accession numbers for these proteins are as follows: NP_010720.1 (ScNpl3), XP_715038.1 (CaNpl3), NP_594570.1 (SpSrp2), CAA22007.1 (CaSlr1), and NP_596398.1 (SpSrp1).

Although CaSlr1 has these structural similarities to SpSrp1, its sequence reveals distinct differences from SpSrp1. Similar to SpSrp2, SpSrp1 contains an additional domain C-terminal to the arginine-rich region (Fig. 1). The amino acid composition of the arginine-rich region of Slr1 more closely resembles those of the Npl3 proteins than that of SpSrp1. In addition, the C terminus of CaSlr1 (RSRSPER) resembles that of ScNpl3 and CaNpl3 (RERSPTR) (identical residues are underlined) (Fig. 1), a known target for ScNpl3 serine phosphorylation (46, 47). In contrast to the Npl3 proteins, however, most of the SR/RS peptides in Slr1 are grouped in a 16-residue region at the C terminus.

Slr1 is more important for *C. albicans* growth than Npl3. To investigate the roles of SR-like proteins in *C. albicans*, strains that lacked Npl3, Slr1, or both proteins were constructed. Wild-type copies of each gene were then reintegrated at their native loci in the homozygous deletion mutants to create reconstituted, heterozygous control strains. In contrast to the importance of Npl3 and Srp2 for growth of *S. cerevisiae* and *S. pombe*, deletion of *CaNPL3* only slightly slowed growth of *C. albicans* in rich medium at 30°C, and the generation time at maximal growth rate for *npl3*Δ/Δ strains was not significantly different from that of a wild-type strain at 37°C (Fig. 2A; see also Fig. S1A in the supplemental material). Deletion of *SLR1*, however, did increase the generation time in YPD broth at both temperatures, with a greater difference from that of the wild type at 37°C (Fig. 2A). *C. albicans* was viable in the absence of both SR-like proteins, and the absence of Npl3 slowed growth of *slr1*Δ/Δ cells at both temperatures (*npl3*Δ/Δ *slr1*Δ/Δ versus *slr1*Δ/Δ: 30°C, $P < 0.01$; 37°C, $P < 0.05$). In addition to altering the maximal growth rate, deletion of *SLR1* increased the lag phase at 37°C but not at 30°C (see Fig. S1B).

To determine whether SR-like proteins affected the stress sensitivity of *C. albicans*, cells were grown at low (16°C) temperature and in the presence of cell membrane and wall stressors, sodium dodecyl sulfate (SDS) and calcofluor white, respectively. Growth of both *npl3*Δ/Δ and *slr1*Δ/Δ mutant strains was reduced at low temperature (see Fig. S2 in the supplemental material), as is seen with many *S. cerevisiae* mutants with defects in RNA processing (48). The *npl3*Δ/Δ mutant did not display increased sensitivity to SDS or calcofluor white, whereas *slr1*Δ/Δ cells were extremely sensitive to both of these stressors (Fig. 2B). The double mutant strain was slightly more sensitive to SDS than the *slr1*Δ/Δ strain. Reconstitution of the double mutant strain with either *SLR1* or *NPL3* resulted in a phenotype equivalent to that of the single mutant strains. Thus, Slr1 is more important than Npl3 for growth of *C. albicans in vitro*, particularly during cell wall and membrane stress.

Slr1 is required for normal hyphal formation. SR-like proteins have been implicated in polar growth of fungi, including the budding yeast *S. cerevisiae* (27, 28) and the filamentous fungus *A. nidulans* (30). We therefore tested the ability of *C. albicans* cells lacking SR-like proteins to filament under different inducing conditions. On solid medium, deletion of *SLR1* decreased filamentous colony growth. Wild-type and *npl3*Δ/Δ cells formed colonies with peripheral filaments on serum and RPMI agar plates, whereas these radiating filaments were absent from *slr1*Δ/Δ colonies (Fig. 3). Cells lacking both SR-like proteins formed colonies similar to *slr1*Δ/Δ colonies on these media (Fig. 3), and reconstitution with wild-type copies of *NPL3* or *SLR1* restored the WT or single mutant phenotypes (Fig. 3).

Filamentation in liquid culture allows the relative speed and

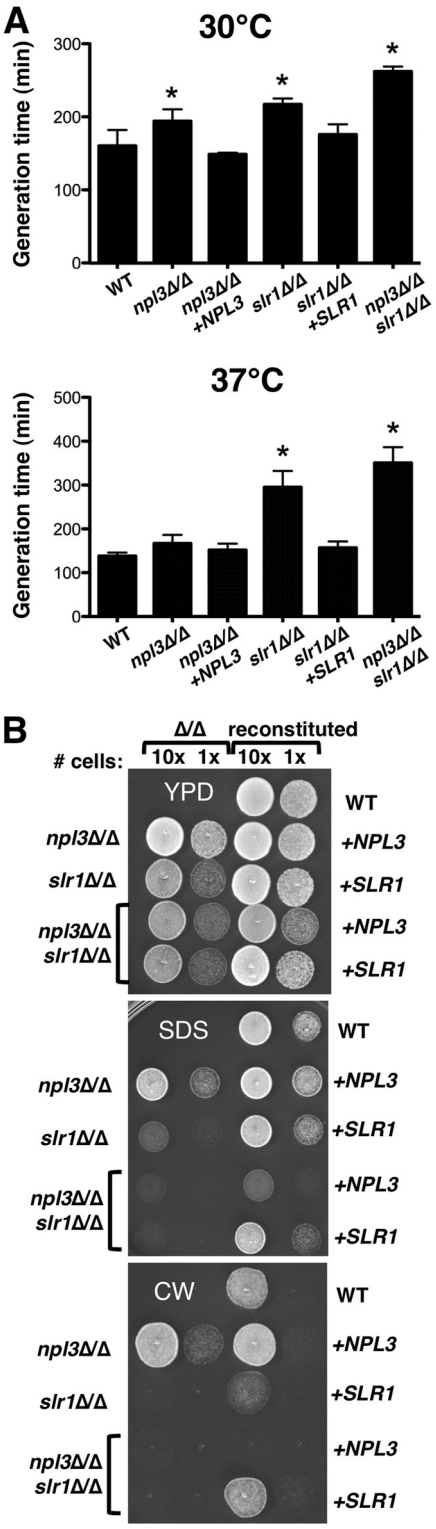

FIG 2 Growth defects associated with *SLR1* deletion in *C. albicans.* (A) Generation times for indicated strains (5 to 10 replicates) were calculated from 24-h growth curves as described in Materials and Methods. Complete genotypes are presented in Table 1. WT, wild type. (B) Two dilutions ($10\times = 5 \times 10^4$ cells; $1\times = 5 \times 10^3$ cells) of strains were grown at 30°C for 1 day on YPD without or with 0.02% SDS or 20 μM calcofluor white (CW). Relevant genotypes of deletion strains tested (2 left spots) are denoted on the left; the wild-type gene reintroduced into each deletion strain to create reconstituted strains (2 right spots) is denoted on the right.

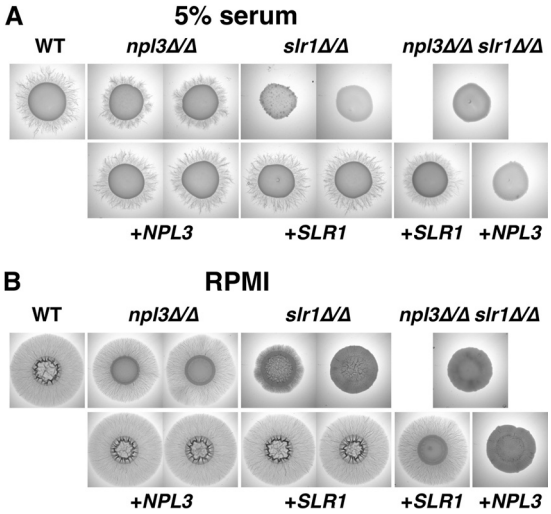

FIG 3 Absence of Slr1 decreases filamentation on solid medium. Stationary-phase cells (10^7) with the indicated genotypes were spotted onto plates containing 5% serum (A) or onto RPMI agar plates (B) and grown for 6 days at 37°C.

form of filamentation to be compared among strains. Although *slr1*Δ/Δ cells showed slower filamentation after incubation in RPMI at 37°C for 1.5 h (Fig. 4A), by 3 h, all strains formed hyphae (Fig. 4B). Cells lacking *NPL3* formed hyphae similar to those of wild-type cells under both conditions (Fig. 4). Thus, Slr1 has a

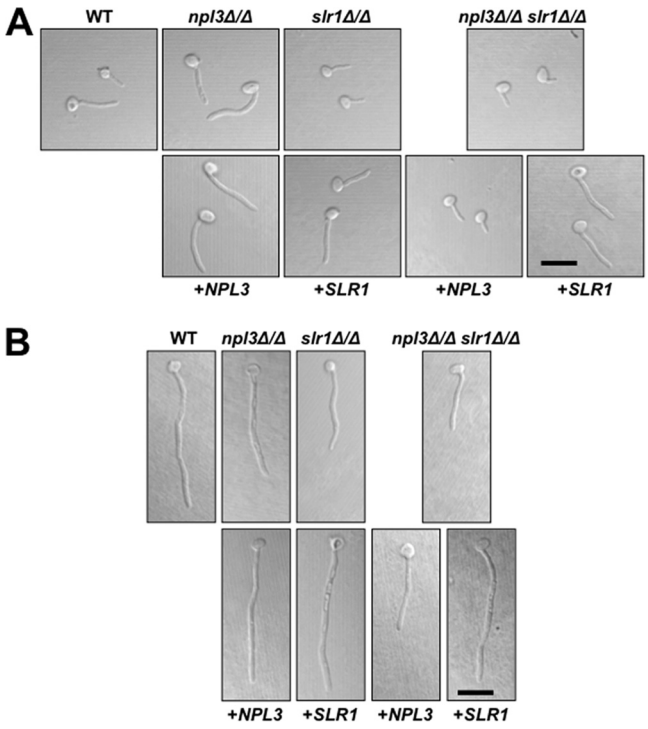

FIG 4 Cells lacking Slr1 can form hyphae in liquid RPMI. Overnight YPD cultures of cells with the indicated genotypes were diluted to 10^5 cells/ml in RPMI and incubated on gelatin-coated coverslips for 1.5 (A) or 3 (B) h at 37°C and 5% CO_2. Paraformaldehyde-fixed cells were imaged by differential interference contrast (DIC) microscopy. Scale bars = 5 μm.

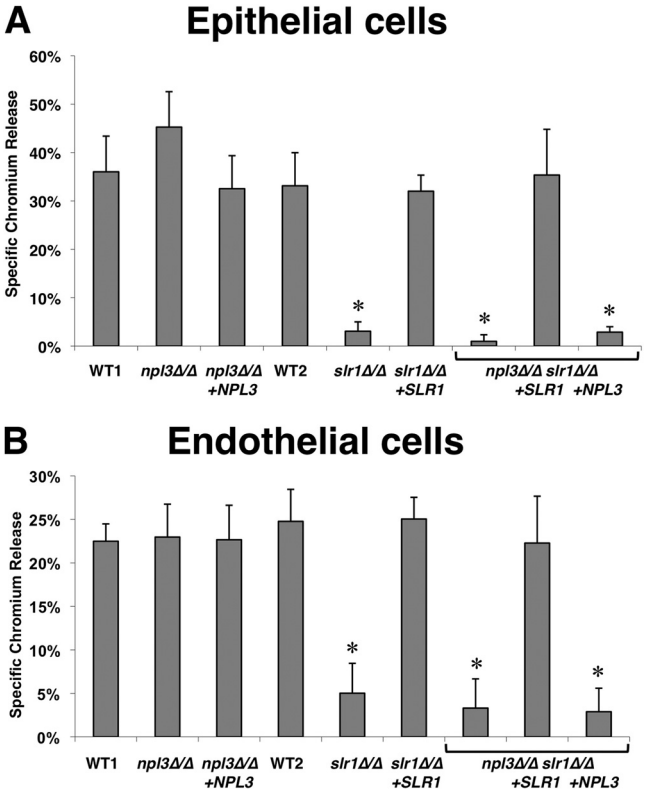

FIG 5 Deletion of *SLR1* decreases cell damage by *C. albicans in vitro*. FaDu oral epithelial cells (A) or human umbilical vein endothelial cells (B) were preloaded with ^{51}Cr and incubated for 3 h at 37°C with the following *C. albicans* strains: the wild type (WT1, DAY185; WT2, AMC81), the *npl3*Δ/Δ mutant (AMC18), the *npl3*Δ/Δ+*NPL3* strain (AMC22), the *slr1*Δ/Δ mutant (AMC82), the *slr1*Δ/Δ+*SLR1* strain (AMC104), the *npl3*Δ/Δ*slr1*Δ/Δ mutant (AMC83), the *npl3*Δ/Δ *slr1*Δ/Δ+*SLR1* strain (AMC111), and the *npl3*Δ/Δ+*NPL3* *slr1*Δ/Δ strain (AMC113). Results are the means ± SD of data from 3 experiments, each performed in triplicate. *, $P < 0.01$ compared to results for the wild type.

stronger effect than Npl3 on *C. albicans* filamentation *in vitro*, and this effect is more pronounced on solid medium.

Deletion of *SLR1* reduces *C. albicans* damage to host cells *in vitro*. Given the effects of *SLR1* and *NPL3* deletion on filamentation, we tested whether these genes also affected interaction of *C. albicans* with the FaDu oral epithelial cell line and HUVECs (49, 50). Whereas the epithelial cell damage caused by *npl3*Δ/Δ cells was slightly but not significantly greater than that induced by wild-type or reconstituted *npl3*Δ/Δ+*NPL3* cells, deletion of *SLR1* significantly decreased the capacity of *C. albicans* to damage oral epithelial cells *in vitro* (Fig. 5A). The epithelial cell damage defect of with *slr1*Δ/Δ was so great that it was not possible to determine if deletion of both *SLR1* and *NPL3* caused a further reduction in damage. *C. albicans*-induced damage to HUVECs was also decreased by deletion of *SLR1* (Fig. 5B). On both epithelial and endothelial cells, mutants in which *SLR1* was deleted grew as a mixture of short true hyphae and pseudohyphae (data not shown). This defect in hyphal formation likely contributed to the reduced damage caused by the *slr1*Δ/Δ mutants. Collectively, these results indicate that *SLR1* but not *NPL3* is required for *C. albicans* to cause maximal damage to host cells *in vitro*.

***SLR1* is important for maximal *C. albicans* virulence during OPC and HDC.** The defects of the *slr1*Δ/Δ mutant in damaging

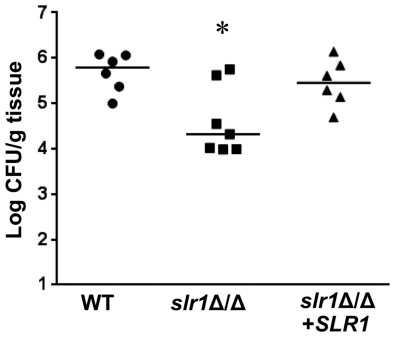

FIG 6 Effects of deletion of *SLR1* on *C. albicans* virulence in the mouse model of OPC. Immunocompromised mice were infected orally with the wild type (AMC81), the *slr1*Δ/Δ mutant (AMC82), or the *slr1*Δ/Δ mutant complemented with *SLR1* (AMC104). The oral fungal burden was determined after 5 days of infection for 6 or 7 mice per strain. Each symbol represents the results for an individual mouse, and the horizontal lines indicate the median values. *, $P = 0.02$ compared to results for the wild-type strain.

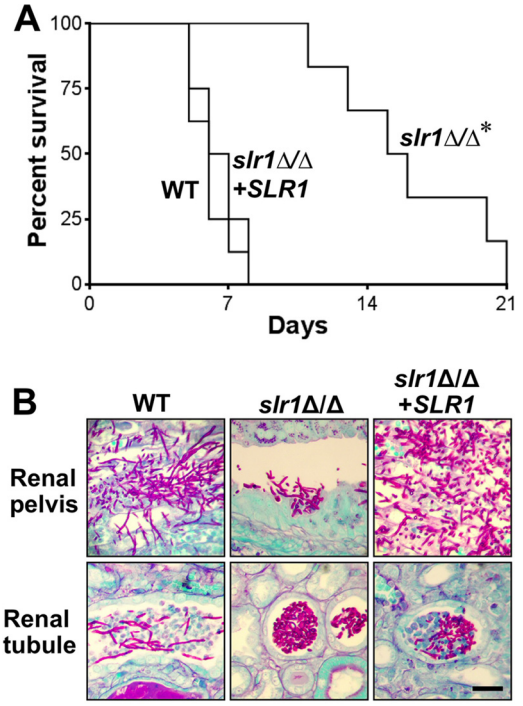

FIG 7 Deletion of *SLR1* affects *C. albicans* virulence, filamentation, and intrakidney localization during disseminated candidiasis. (A) Survival of mice injected intravenously with the wild type (AMC81), the *slr1*Δ/Δ mutant (AMC82), or the *slr1*Δ/Δ mutant complemented with *SLR1* (AMC104). Each strain was injected into 8 mice, and host survival was monitored over a 3-week period. *, $P < 0.0001$ versus results for other strains. (B) Histopathology of kidney sections after 4 days of infection with the indicated strains. Sections were stained with periodic acid-Schiff stain. Scale bar = 20 μm.

oral epithelial cells and HUVECs suggested that this mutant would have attenuated virulence in animal models of infection (41). To test this hypothesis, the virulence of the wild-type strain, the *slr1*Δ/Δ mutant, and the *slr1*Δ/Δ+*SLR1* reconstituted strain was tested in mouse models of OPC and HDC. In the OPC model, the median oral fungal burden of mice infected with the *slr1*Δ/Δ mutant was more than 10-fold lower than that of mice infected with either the homozygous *SLR1*/*SLR1* wild-type strain or the *slr1*Δ/Δ+*SLR1* reconstituted strain (Fig. 6). However, this reduction in oral fungal burden in the mice infected with the *slr1*Δ/Δ mutant was statistically significant compared with that of mice infected with the wild-type strain ($P = 0.02$) but not the *slr1*Δ/Δ+*SLR1* reconstituted strain ($P = 0.07$). The oral fungal burden in mice infected with wild-type and reconstituted strains was not significantly different ($P = 0.48$).

In the HDC model, the median survival of mice injected with the *slr1*Δ/Δ mutant was more than twice as long as that of mice infected with either the wild-type strain or the *slr1*Δ/Δ+*SLR1* reconstituted strain (Fig. 7A). Therefore, *SLR1* is necessary for maximal virulence during HDC. To verify this finding, we repeated the survival experiment with a second, independent pair of *slr1*Δ/Δ mutant and *slr1*Δ/Δ+*SLR1* reconstituted strains and obtained similar results (see Fig. S3 in the supplemental material). These data indicate that the presence of Slr1 affects expression of genes that are important for virulence during HDC.

To determine whether the attenuated virulence of the *slr1*Δ/Δ mutant in the HDC model was solely due to slow growth *in vivo*, the organ fungal burden was determined 4 days postinfection. Although the *slr1*Δ/Δ mutant grew slower than the wild-type strain *in vitro* (Fig. 2A), the kidney and liver fungal burdens of mice infected with the *slr1*Δ/Δ strain were similar to those of mice infected with the wild-type strain (see Fig. S4 in the supplemental material). Therefore, the virulence defect of the *slr1*Δ/Δ mutant did not appear to be the result of impaired growth *in vivo*.

Next, we performed histopathologic analysis of thin sections of the infected kidneys from three mice to determine effects of *SLR1* deletion on *C. albicans* filamentation. As expected, the wild-type cells formed extensive filaments in both the renal pelvis and renal tubules (Fig. 7B). In contrast, although the *slr1*Δ/Δ cells formed some filaments in the renal pelvis, they grew as large aggregates of yeast in the renal tubules. The morphology of *C. albicans* cells containing a single reintroduced copy of *SLR1* was intermediate to that of the wild-type strain and the *slr1*Δ/Δ mutant. These results indicate that *SLR1* influences the capacity of *C. albicans* to form hyphae within the renal tubules but not within the renal pelvis.

The *slr1*Δ/Δ mutant had increased tropism for the brain. Interestingly, the brain fungal burden of mice infected with the *slr1*Δ/Δ strain was significantly higher than that of either the wild type or the reconstituted strain (Fig. 8A). This result suggested that deletion of *SLR1* might increase the interaction of *C. albicans* with the unique endothelial cells that line the blood vessels of the brain. We therefore compared the capacity of the *slr1*Δ/Δ mutant to invade HBMECs, representative of brain endothelial cells, and HUVECs, representative of systemic endothelial cells. We found that the *slr1*Δ/Δ mutant had significantly increased invasion of HBMECs compared to that of the wild-type and reconstituted strains (Fig. 8B). In contrast, the *slr1*Δ/Δ mutant had significantly impaired invasion of HUVECs. Thus, it is probable that the increased capacity of the *slr1*Δ/Δ mutant to invade brain endothelial cells contributed to the elevated brain fungal burdens in mice infected with this strain.

Interestingly, although the *slr1*Δ/Δ mutant had enhanced invasion of HBMECs, it still caused significantly less damage to these endothelial cells than the wild-type and reconstituted strains (Fig. 8C). These results suggest that brain endothelial cell invasion, rather than damage, is an important determinant of brain tropism.

We have found previously that a *vps51*Δ/Δ mutant also has

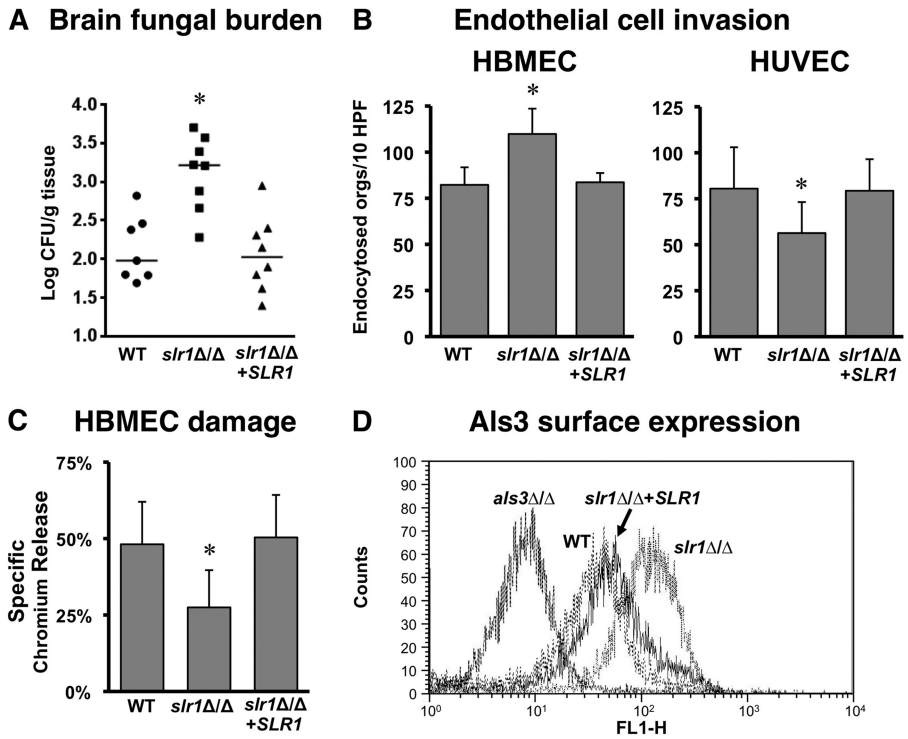

FIG 8 Deletion of *SLR1* increases brain tropism of *C. albicans.* (A) Deletion of *SLR1* increases fungal burden in the brain. Brain fungal burdens of mice 4 days after intravenous inoculation with the wild-type (AMC81), *slr1*Δ/Δ (AMC82), or *slr1*Δ/Δ+*SLR1* (AMC104) strain are shown. Each symbol represents the results for an individual mouse, and the horizontal lines indicate the median values. *, $P < 0.005$ compared to results for the wild-type and reconstituted strains. (B and C) The strains in panel A were tested for invasion of HBMECs and HUVECs after 3 h of incubation (B) and for their capacity to cause HBMEC damage after 16 h of infection (C). Results are the means ± SD for 3 experiments, each performed in triplicate. *, $P \leq 0.02$ versus results for the wild-type and reconstituted strains. (D) Level of surface expression of Als3 for the indicated strains as assessed by flow cytometry. Abbreviations: orgs, oganisms; HPF, high-powered field.

increased capacity to invade HBMECs *in vitro* and traffic to the brain in the mouse model of HDC. This enhanced trafficking is due in part to increased expression of the Als3 invasin on the surface of the *vps51*Δ/Δ mutant (39). Interestingly, flow cytometric analysis revealed that *slr1*Δ/Δ germ tubes also had greater surface expression of Als3 than those of the wild-type and reconstituted strains. This enhanced expression of Als3 likely contributes to the increased trafficking of the *slr1*Δ/Δ mutant to the brain.

DISCUSSION

To date, studies of how gene expression influences *C. albicans* hyphal development and function have focused primarily on transcriptional and posttranslational signaling mechanisms (9). The prevalence of posttranscriptional processes that control polar growth in other eukaryotic systems (14–16) led us to examine the roles of two RNA-binding proteins encoded in the *C. albicans* genome, Npl3 and Slr1. Orthologs of *NPL3* had previously been identified as essential genes in *S. cerevisiae* and *S. pombe* (51–53), and a transposon mutagenesis screen for *S. cerevisiae* genes required for the switch from budding to pseudohyphal growth implicated *NPL3* in polar growth (28). In contrast, we found that *C. albicans* cells lacking *NPL3* grew as robustly as wild-type cells at 37°C and displayed wild-type hyphal formation. These results were consistent with those of Bonhomme and colleagues: deletion of *NPL3* did not affect hyphal formation on RPMI agar, in liquid Lee's medium, and under embedded conditions (54). The absence of *SLR1*, however, slowed growth at 37°C, increased sensitivity to cell wall and membrane stresses, altered filamentation on both serum and RPMI agar medium, and retarded germ tube elongation in liquid medium. Although the *S. cerevisiae* genome does not encode an apparent ortholog of *SLR1*, *SLR1* gene structure and the predicted Slr1 RNA recognition motif sequence suggest an evolutionary relationship with Srp1, a nonessential SR-like protein in *S. pombe*, and SwoK in the filamentous fungus *A. nidulans*. SwoK was identified in a screen for cells with a "swollen" phenotype upon conidial germination at the restrictive temperature, indicating a switch from the polarized growth required for mycelium formation to isotropic growth (30). The filamentation phenotypes of *slr1*Δ/Δ *C. albicans* cells and the *swoK1 A. nidulans* mutant suggest the importance of this family of RNA-binding proteins for polar growth in multiple fungi.

Previous studies in *C. albicans* have linked filamentous growth to RNA-binding proteins involved in mRNA turnover and transport. Similar to Slr1, the 5′-to-3′ exonuclease Kem1, which degrades mRNAs following decapping, the deadenylase complex proteins Ccr4 and Pop2, and the mRNA-binding protein She3, which helps localize multiple mRNAs to the hyphal tip, are all required for peripheral filaments to form around colonies grown on solid Spider medium (10, 12, 13). Although hyphal formation has been linked to virulence, a recent large-scale study of strains with deletions in 674 genes has shown that almost half of all strains with attenuated infectivity in a mouse model of hematogenously disseminated candidiasis have no *in vitro* proliferation or filamentation defect on Spider medium (55). Conversely, two-thirds of

the mutant strains with the strongest morphology defects *in vitro* still infected mice as well as the wild-type strain (55). Therefore, filamentation defects *in vitro* do not necessarily result in virulence defects *in vivo*. We found that the *slr1*Δ/Δ mutant had attenuated virulence in the mouse model of HDC. A *ccr4*Δ/Δ mutant also has attenuated virulence in this model system (13), whereas a *she3*Δ/Δ mutant has normal virulence in mice (12). Although the *kem1*Δ/Δ mutant has not been tested in this model, this mutant does have lower virulence in a *Galleria mellonella* model of infection (56).

The attenuated virulence of the *slr1*Δ/Δ mutant was likely multifactorial. This strain had impaired capacity to damage both endothelial and epithelial cells *in vitro*, a phenotype that has been associated with virulence defects in mouse models of candidiasis (40, 41). It is probable that the filamentation defect of *slr1*Δ/Δ cells in the kidney also contributed to its attenuated virulence. Furthermore, there were interesting differences in the localization of this mutant within different regions of the kidney. There was a greater number of *slr1*Δ/Δ yeast cells than wild-type cells in the renal tubules and a smaller number of *slr1*Δ/Δ hyphae than wild-type cells in the renal pelvis (Fig. 7B). Reconstituted cells with a single copy of *SLR1* showed an intermediate phenotype. The high density of *slr1*Δ/Δ yeast in the tubules also raises the question of whether these yeast-form *slr1*Δ/Δ cells might be retained in the tubule or otherwise unable to progress to the renal pelvis. A similar phenomenon—equivalent kidney fungal burdens compared to those for wild-type cells with differences in morphology and intrakidney localization—was seen for *C. albicans* lacking the Rsr1 GTPase, which plays a role in hyphal tip orientation (57).

Although the *slr1*Δ/Δ mutant grew slowly *in vitro*, the kidney fungal burden of mice infected with this strain was similar to that of mice infected with the wild-type strain. Noble and colleagues similarly found that numerous mutants with growth defects *in vitro* achieved normal fungal density in the kidney when inoculated into mice (55). Therefore, the impaired growth of the *slr1*Δ/Δ mutant likely played a minor role in its reduced virulence in the mouse model of HDC. However, in the mouse model of OPC, the *slr1*Δ/Δ mutant achieved a lower oral fungal burden than did the wild-type strain. Based on our *in vitro* data, the impaired virulence of the *slr1*Δ/Δ mutant was likely due a combination of slower growth in the oropharynx and a reduced capacity to damage oral epithelial cells.

An unexpected finding was that the absence of *SLR1* led to an increased fungal burden in the brain. This tropism suggests that Slr1 might affect the expression of genes involved in interactions with brain endothelial cells. Indeed, whereas deletion of *SLR1* decreased the endocytosis of *C. albicans* by HUVECs, it significantly increased endocytosis by HBMECs. Recently, a similar tropism was found for *C. albicans* lacking the putative vacuolar sorting protein Vps51 (39). In the mouse models of HDC, the brain fungal burden of mice infected with a *vps51*Δ/Δ mutant was significantly greater than that of mice infected with a wild-type strain. In addition, although *vps51*Δ/Δ cells were poorly endocytosed by HUVECs, they were endocytosed more avidly than wild-type cells by HBMECs. Endocytosis of *C. albicans* by brain endothelial cells was found to be mediated in part by the binding of cell-wall-associated Als3 to heat shock protein gp96 on host cells; the brain tropism of the *vps51*Δ/Δ mutant resulted from greater exposure of Als3 on the *C. albicans* cell surface (39). We found that deletion of *SLR1* also resulted in increased surface exposure of Als3, thus providing a potential mechanism for the brain tropism of *slr1*Δ/Δ cells.

Whereas studies of other fungal RNA-binding proteins indicate that numerous posttranscriptional steps in gene expression can affect polar growth and cell surface processes (12, 13, 16, 58), the mechanism(s) whereby Slr1 directly or indirectly affects filamentation and interactions with host cells remains to be determined. Future work to understand how Slr1 impacts *C. albicans* hyphal growth and virulence will focus on identifying its mRNA targets and how it influences their expression and localization during hyphal growth.

ACKNOWLEDGMENTS

This project was supported by the National Institutes of Health, grants 5P20RR016463, 8P20GM103423, 2R01AI054928, and 2R01DE017088. The umbilical cords used in this study were collected by the pediatric, perinatal, and mobile unit of the UCLA Clinical and Translational Science Institute at LA BioMed/Harbor-UCLA Medical Center, funded by the National Center for Advancing Translational Sciences, grant UL1TR000124. This project was also supported by grants from the National Center for Research Resources (5P20RR016463) and the National Institute of General Medical Sciences (8 P20 GM103423) from the National Institutes of Health. C.A. was supported by undergraduate research fellowships from the American Society for Microbiology and the Howard Hughes Medical Institute.

We thank Aaron Mitchell for reagents, Anja Forche for critical reading of the manuscript and technical advice, and Darren Abbey and Sven Bergmann for providing growth curve analysis software prior to publication.

REFERENCES

1. **Wisplinghoff H, Bischoff T, Tallent SM, Seifert H, Wenzel RP, Edmond MB.** 2004. Nosocomial bloodstream infections in US hospitals: analysis of 24,179 cases from a prospective nationwide surveillance study. Clin. Infect. Dis. **39**:309–317.
2. **Lo HJ, Kohler JR, DiDomenico B, Loebenberg D, Cacciapuoti A, Fink GR.** 1997. Nonfilamentous *C. albicans* mutants are avirulent. Cell **90**:939–949.
3. **Saville SP, Lazzell AL, Monteagudo C, Lopez-Ribot JL.** 2003. Engineered control of cell morphology *in vivo* reveals distinct roles for yeast and filamentous forms of *Candida albicans* during infection. Eukaryot. Cell **2**:1053–1060.
4. **Filler SG, Sheppard DC.** 2006. Fungal invasion of normally non-phagocytic host cells. PLoS Pathog. **2**:e129. doi:10.1371/journal.ppat.0020129.
5. **Nantel A, Dignard D, Bachewich C, Harcus D, Marcil A, Bouin AP, Sensen CW, Hogues H, van het Hoog M, Gordon P, Rigby T, Benoit F, Tessier DC, Thomas DY, Whiteway M.** 2002. Transcription profiling of *Candida albicans* cells undergoing the yeast-to-hyphal transition. Mol. Biol. Cell **13**:3452–3465.
6. **Kadosh D, Johnson AD.** 2005. Induction of the *Candida albicans* filamentous growth program by relief of transcriptional repression: a genome-wide analysis. Mol. Biol. Cell **16**:2903–2912.
7. **Sellam A, Hogues H, Askew C, Tebbji F, van Het Hoog M, Lavoie H, Kumamoto CA, Whiteway M, Nantel A.** 2010. Experimental annotation of the human pathogen *Candida albicans* coding and noncoding transcribed regions using high-resolution tiling arrays. Genome Biol. **11**:R71. doi:10.1186/gb-2010-11-7-r71.
8. **Bruno VM, Wang Z, Marjani SL, Euskirchen GM, Martin J, Sherlock G, Snyder M.** 2010. Comprehensive annotation of the transcriptome of the human fungal pathogen *Candida albicans* using RNA-seq. Genome Res. **20**:1451–1458.
9. **Whiteway M, Bachewich C.** 2007. Morphogenesis in *Candida albicans*. Annu. Rev. Microbiol. **61**:529–553.
10. **An HS, Lee KH, Kim J.** 2004. Identification of an exoribonuclease homolog, CaKEM1/CaXRN1, in *Candida albicans* and its characterization in filamentous growth. FEMS Microbiol. Lett. **235**:297–303.
11. **Richard ML, Nobile CJ, Bruno VM, Mitchell AP.** 2005. *Candida albicans* biofilm-defective mutants. Eukaryot. Cell **4**:1493–1502.
12. **Elson SL, Noble SM, Solis NV, Filler SG, Johnson AD.** 2009. An RNA transport system in *Candida albicans* regulates hyphal morphology and invasive growth. PLoS Genet. **5**:e1000664. doi:10.1371/journal.pgen.1000664.

13. **Dagley MJ, Gentle IE, Beilharz TH, Pettolino FA, Djordjevic JT, Lo TL, Uwamahoro N, Rupasinghe T, Tull DL, McConville M, Beaurepaire C, Nantel A, Lithgow T, Mitchell AP, Traven A.** 2011. Cell wall integrity is linked to mitochondria and phospholipid homeostasis in *Candida albicans* through the activity of the post-transcriptional regulator Ccr4-Pop2. Mol. Microbiol. **79**:968–989.
14. **Lasko P.** 2011. Posttranscriptional regulation in Drosophila oocytes and early embryos. Wiley Interdiscip. Rev. RNA **2**:408–416.
15. **Donnelly CJ, Fainzilber M, Twiss JL.** 2010. Subcellular communication through RNA transport and localized protein synthesis. Traffic **11**:1498–1505.
16. **Vollmeister E, Feldbrugge M.** 2010. Posttranscriptional control of growth and development in *Ustilago maydis*. Curr. Opin. Microbiol. **13**: 693–699.
17. **Tuch BB, Mitrovich QM, Homann OR, Hernday AD, Monighetti CK, De La Vega FM, Johnson AD.** 2010. The transcriptomes of two heritable cell types illuminate the circuit governing their differentiation. PLoS Genet. **6**:e1001070. doi:10.1371/journal.pgen.1001070.
18. **Shepard PJ, Hertel KJ.** 2009. The SR protein family. Genome Biol. **10**:242. doi:10.1186/gb-2009-10-10-242.
19. **Long JC, Caceres JF.** 2009. The SR protein family of splicing factors: master regulators of gene expression. Biochem. J. **417**:15–27.
20. **Zhong XY, Wang P, Han J, Rosenfeld MG, Fu XD.** 2009. SR proteins in vertical integration of gene expression from transcription to RNA processing to translation. Mol. Cell **35**:1–10.
21. **Kress TL, Krogan NJ, Guthrie C.** 2008. A single SR-like protein, Npl3, promotes pre-mRNA splicing in budding yeast. Mol. Cell **32**:727–734.
22. **Dermody JL, Dreyfuss JM, Villen J, Ogundipe B, Gygi SP, Park PJ, Ponticelli AS, Moore CL, Buratowski S, Bucheli ME.** 2008. Unphosphorylated SR-like protein Npl3 stimulates RNA polymerase II elongation. PLoS One **3**:e3273. doi:10.1371/journal.pone.0003273.
23. **Bucheli ME, Buratowski S.** 2005. Npl3 is an antagonist of mRNA 3′ end formation by RNA polymerase II. EMBO J. **24**:2150–2160.
24. **Kadowaki T, Chen S, Hitomi M, Jacobs E, Kumagai C, Liang S, Schneiter R, Singleton D, Wisniewska J, Tartakoff AM.** 1994. Isolation and characterization of *Saccharomyces cerevisiae* mRNA transport-defective (mtr) mutants. J. Cell Biol. **126**:649–659.
25. **Lee MS, Henry M, Silver PA.** 1996. A protein that shuttles between the nucleus and the cytoplasm is an important mediator of RNA export. Genes Dev. **10**:1233–1246.
26. **Windgassen M, Sturm D, Cajigas IJ, Gonzalez CI, Seedorf M, Bastians H, Krebber H.** 2004. Yeast shuttling SR proteins Npl3p, Gbp2p, and Hrb1p are part of the translating mRNPs, and Npl3p can function as a translational repressor. Mol. Cell. Biol. **24**:10479–10491.
27. **Ni L, Snyder M.** 2001. A genomic study of the bipolar bud site selection pattern in *Saccharomyces cerevisiae*. Mol. Biol. Cell **12**:2147–2170.
28. **Mosch HU, Fink GR.** 1997. Dissection of filamentous growth by transposon mutagenesis in *Saccharomyces cerevisiae*. Genetics **145**:671–684.
29. **McBride AE, Zurita-Lopez C, Regis A, Blum E, Conboy A, Elf S, Clarke S.** 2007. Protein arginine methylation in *Candida albicans*: role in nuclear transport. Eukaryot. Cell **6**:1119–1129.
30. **Shaw BD, Upadhyay S.** 2005. *Aspergillus nidulans swoK* encodes an RNA binding protein that is important for cell polarity. Fungal Genet. Biol. **42**:862–872.
31. **Wilson RB, Davis D, Mitchell AP.** 1999. Rapid hypothesis testing with *Candida albicans* through gene disruption with short homology regions. J. Bacteriol. **181**:1868–1874.
32. **Lay J, Henry LK, Clifford J, Koltin Y, Bulawa CE, Becker JM.** 1998. Altered expression of selectable marker *URA3* in gene-disrupted *Candida albicans* strains complicates interpretation of virulence studies. Infect. Immun. **66**:5301–5306.
33. **Ketel C, Wang HS, McClellan M, Bouchonville K, Selmecki A, Lahav T, Gerami-Nejad M, Berman J.** 2009. Neocentromeres form efficiently at multiple possible loci in *Candida albicans*. PLoS Genet. **5**:e1000400. doi: 10.1371/journal.pgen.1000400.
34. **Zwietering MH, Jongenburger I, Rombouts FM, Kvan 't Riet.** 1990. Modeling of the bacterial growth curve. Appl. Environ. Microbiol. **56**: 1875–1881.
35. **Liu H, Kohler J, Fink GR.** 1994. Suppression of hyphal formation in *Candida albicans* by mutation of a STE12 homolog. Science **266**:1723–1726.
36. **Jaffe EA, Nachman RL, Becker CG, Minick CR.** 1973. Culture of human endothelial cells derived from umbilical veins. Identification by morphologic and immunologic criteria. J. Clin. Invest. **52**:2745–2756.
37. **Phan QT, Myers CL, Fu Y, Sheppard DC, Yeaman MR, Welch WH, Ibrahim AS, Edwards JE, Jr, Filler SG.** 2007. Als3 is a *Candida albicans* invasin that binds to cadherins and induces endocytosis by host cells. PLoS Biol. **5**:e64. doi:10.1371/journal.pbio.0050064.
38. **Stins MF, Nemani PV, Wass C, Kim KS.** 1999. *Escherichia coli* binding to and invasion of brain microvascular endothelial cells derived from humans and rats of different ages. Infect. Immun. **67**:5522–5525.
39. **Liu Y, Mittal R, Solis NV, Prasadarao NV, Filler SG.** 2011. Mechanisms of *Candida albicans* trafficking to the brain. PLoS Pathog. **7**:e1002305. doi:10.1371/journal.ppat.1002305.
40. **Park H, Myers CL, Sheppard DC, Phan QT, Sanchez AA, Edwards JE, Filler SG.** 2005. Role of the fungal Ras-protein kinase A pathway in governing epithelial cell interactions during oropharyngeal candidiasis. Cell Microbiol. **7**:499–510.
41. **Sanchez AA, Johnston DA, Myers C, Edwards JE, Jr, Mitchell AP, Filler SG.** 2004. Relationship between *Candida albicans* virulence during experimental hematogenously disseminated infection and endothelial cell damage *in vitro*. Infect. Immun. **72**:598–601.
42. **Kamai Y, Kubota M, Hosokawa T, Fukuoka T, Filler SG.** 2001. New model of oropharyngeal candidiasis in mice. Antimicrob. Agents Chemother. **45**:3195–3197.
43. **Solis NV, Filler SG.** 2012. Mouse model of oropharyngeal candidiasis. Nat. Protoc. **7**:637–642.
44. **Phan QT, Fratti RA, Prasadarao NV, Edwards JE, Jr, Filler SG.** 2005. N-cadherin mediates endocytosis of *Candida albicans* by endothelial cells. J. Biol. Chem. **280**:10455–10461.
45. **Plass M, Agirre E, Reyes D, Camara F, Eyras E.** 2008. Co-evolution of the branch site and SR proteins in eukaryotes. Trends Genet. **24**:590–594.
46. **Gilbert W, Siebel CW, Guthrie C.** 2001. Phosphorylation by Sky1p promotes Npl3p shuttling and mRNA dissociation. RNA **7**:302–313.
47. **Yun CY, Fu XD.** 2000. Conserved SR protein kinase functions in nuclear import and its action is counteracted by arginine methylation in *Saccharomyces cerevisiae*. J. Cell Biol. **150**:707–718.
48. **Aguilera J, Randez-Gil F, Prieto JA.** 2007. Cold response in *Saccharomyces cerevisiae*: new functions for old mechanisms. FEMS Microbiol. Rev. **31**:327–341.
49. **Zhu W, Filler SG.** 2010. Interactions of *Candida albicans* with epithelial cells. Cell Microbiol. **12**:273–282.
50. **Phan QT, Belanger PH, Filler SG.** 2000. Role of hyphal formation in interactions of *Candida albicans* with endothelial cells. Infect. Immun. **68**:3485–3490.
51. **Bossie MA, DeHoratius C, Barcelo G, Silver P.** 1992. A mutant nuclear protein with similarity to RNA binding proteins interferes with nuclear import in yeast. Mol. Biol. Cell **3**:875–893.
52. **Russell ID, Tollervey D.** 1992. NOP3 is an essential yeast protein which is required for pre-rRNA processing. J. Cell Biol. **119**:737–747.
53. **Lutzelberger M, Gross T, Kaufer NF.** 1999. Srp2, an SR protein family member of fission yeast: *in vivo* characterization of its modular domains. Nucleic Acids Res. **27**:2618–2626.
54. **Bonhomme J, Chauvel M, Goyard S, Roux P, Rossignol T, d'Enfert C.** 2011. Contribution of the glycolytic flux and hypoxia adaptation to efficient biofilm formation by *Candida albicans*. Mol. Microbiol. **80**:995–1013.
55. **Noble SM, French S, Kohn LA, Chen V, Johnson AD.** 2010. Systematic screens of a *Candida albicans* homozygous deletion library decouple morphogenetic switching and pathogenicity. Nat. Genet. **42**:590–598.
56. **Fuchs BB, Eby J, Nobile CJ, El Khoury JB, Mitchell AP, Mylonakis E.** 2010. Role of filamentation in *Galleria mellonella* killing by *Candida albicans*. Microbes Infect. **12**:488–496.
57. **Brand A, Vacharaksa A, Bendel C, Norton J, Haynes P, Henry-Stanley M, Wells C, Ross K, Gow NA, Gale CA.** 2008. An internal polarity landmark is important for externally induced hyphal behaviors in *Candida albicans*. Eukaryot. Cell **7**:712–720.
58. **Wolf JJ, Dowell RD, Mahony S, Rabani M, Gifford DK, Fink GR.** 2010. Feed-forward regulation of a cell fate determinant by an RNA-binding protein generates asymmetry in yeast. Genetics **185**:513–522.
59. **Davis D, Edwards JE, Jr, Mitchell AP, Ibrahim AS.** 2000. *Candida albicans* RIM101 pH response pathway is required for host-pathogen interactions. Infect. Immun. **68**:5953–5959.